Theoretical and experimental study of the catalytic cathodic stripping square-wave voltammetry of chromium species
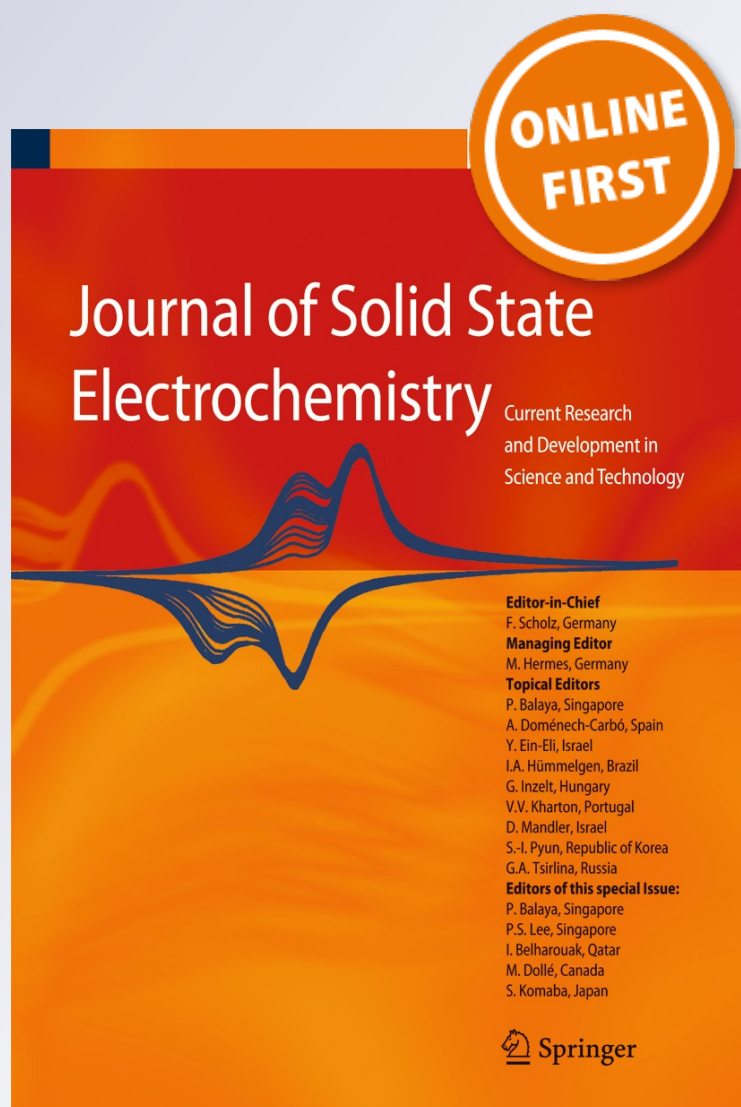
Mariela Cuéllar, Sabrina N. Vettorelo, Patricia I. Ortiz & Fernando Garay

ONLINE FIRST

Journal of Solid State Electrochemistry

Current Research and Development in Science and Technology

Springer

Springer

CrossMark

Theoretical and experimental study of the catalytic cathodic stripping square-wave voltammetry of chromium species

Mariela Cuéllar[1,2] · Sabrina N. Vettorelo[1,2] · Patricia I. Ortiz[1,2] · Fernando Garay[1,2]

Abstract The electrocatalytic mechanism of Cr(III) reduction in the presence of diethylenetriaminepentaacetic acid (DTPA) and nitrate ions is studied theoretically and experimentally by using stripping square-wave voltammetry (SWV). Experimental curves are in excellent agreement with theoretical profiles corresponding to a catalytic reaction of second kind. This type of mechanism is equivalent to a CE mechanism, where the chemical reaction produces the electroactive species. Accordingly, the reaction of Cr(III)–H_2O–DTPA and NO_3^- would produce the electroactive species Cr(III)–NO_3–DTPA and this last species would release NO_2^- to the solution during the electrochemical step. In this regard, the complex of Cr(III)–DTPA would work as the catalyzer that allows the reduction of NO_3^- to NO_2^-. Furthermore, it was found that the electrochemical reaction is quite irreversible, with a constant of $k_s = 9.4 \times 10^{-5}$ cm s^{-1}, while the constant for the chemical step has been estimated to be $k_{chem} = 1.3 \times 10^4$ s^{-1}. Considering that the equilibrium constant is $K = 0.01$, it is possible to estimate the kinetic constants of the chemical reaction as $k_1 = 1 \times 10^2$ s^{-1} and $k_{-1} = 1.29 \times 10^4$ s^{-1}. These values of k_1 and k_{-1} indicate that the exchange of water molecules by nitrate is fast and that the equilibrium favors the complex with

water. Also, a value for the formal potential $E^{o'} \approx -1.1$ V was obtained. The model used for simulating experimental curves does not consider the adsorption of reactants yet. Accordingly, weak adsorption of reagents should be expected.

Keywords Square-wave voltammetry · Catalytic · Mathematical modelling · DTPA · CE mechanism · Cr speciation · Catalysis of second type

Introduction

Nowadays, catalytic electrochemical reactions are of central attention in voltammetric analysis. This is because they provide the possibility for developing highly sensitive strategies for quantitative determination [1–8]. Incidentally, catalytic cathodic stripping voltammetry (CCSV) has proved to be useful for quantifying Cr(VI) in some natural waters with detection limits below the nanomolar level [1, 2, 10, 11]. The toxicity of Cr species strongly depends on its oxidation state. Cr(VI) is a carcinogenic specie which is obviously toxic for humans, while trace levels of Cr(III) are required as mineral supplement of our diet [1, 10, 11]. Thus, speciation of Cr is necessary to assess its ecological impact as well as its mobility through the environment. Several efforts have been done in this regard. Particularly CCSV has been applied to study the reaction of Cr(VI) and Cr(III) species in the presence of diethylenetriaminepentaacetic acid (DTPA) [1, 4, 10–14]. Irrespectively of the chromium oxidation state, the peak current has been assigned to the reduction of Cr(III)–DTPA to Cr(II)–DTPA at a mercury drop surface.

DTPA is a chelating agent that forms very stable complexes with several transition-metal cations [4, 11, 15]. This ligand has eight acid-base equilibria that define the relative concentrations of the cationic, neutral, and anionic species of DTPA
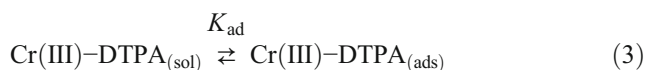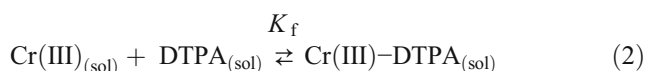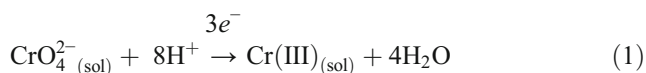
✉ Fernando Garay
  fsgaray@gmail.com

1 INFIQC-CONICET, Departamento de Físico Química, Facultad de Ciencias Químicas, Universidad Nacional de Córdoba, X5000HUA Córdoba, Argentina

2 Pabellón Argentina, Ciudad Universitaria, X5000HUA Córdoba, Argentina
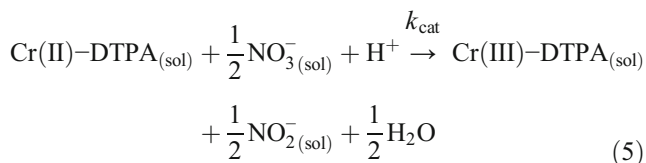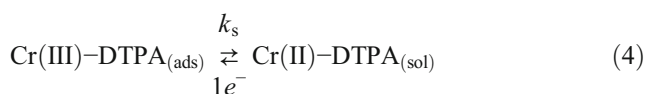
Springer

at a given pH, as well as the diverse kind of complexes that can be formed with metal cations. In the case of Cr(III), all complexes have stoichiometry 1:1 and their remarkable stability can be inferred from the stability constants $\beta_{\text{CrDTPA}} = 1.1 \times 10^{22}$, $\beta_{\text{CrDTPAH}} = 1.5 \times 10^{28}$, $\beta_{\text{CrDTPAH2}} = 1.1 \times 10^{31}$, and $\beta_{\text{CrDTPAH3}} = 3.0 \times 10^{32}$ [15].

The electrochemical reaction of Cr(VI) and Cr(III) species in the presence of DTPA and nitrate ions can be described according to the following set of equations [11]:

For $-1.2 \text{ V} < E < -1.0 \text{ V}$:

$$\text{CrO}_4^{2-}{}_{\text{(sol)}} + 8\text{H}^+ \xrightarrow{3e^-} \text{Cr(III)}_{\text{(sol)}} + 4\text{H}_2\text{O} \tag{1}$$

$$\text{Cr(III)}_{\text{(sol)}} + \text{DTPA}_{\text{(sol)}} \overset{K_f}{\rightleftarrows} \text{Cr(III)}{-}\text{DTPA}_{\text{(sol)}} \tag{2}$$

$$\text{Cr(III)}{-}\text{DTPA}_{\text{(sol)}} \overset{K_{ad}}{\rightleftarrows} \text{Cr(III)}{-}\text{DTPA}_{\text{(ads)}} \tag{3}$$

For $-1.5 \text{ V} < E < -1.2 \text{ V}$:

$$\text{Cr(III)}{-}\text{DTPA}_{\text{(ads)}} \overset{k_s}{\underset{1e^-}{\rightleftarrows}} \text{Cr(II)}{-}\text{DTPA}_{\text{(sol)}} \tag{4}$$

$$\text{Cr(II)}{-}\text{DTPA}_{\text{(sol)}} + \frac{1}{2}\text{NO}_3^-{}_{\text{(sol)}} + \text{H}^+ \xrightarrow{k_{cat}} \text{Cr(III)}{-}\text{DTPA}_{\text{(sol)}}$$
$$+ \frac{1}{2}\text{NO}_2^-{}_{\text{(sol)}} + \frac{1}{2}\text{H}_2\text{O} \tag{5}$$

Eqs. (1, 2 and 3) take place during the accumulation step, while Eqs. (4, 5) correspond to the so-called catalytic mechanism of first kind [9]. The latter can be rewritten in a general form as:

$$O_{\text{(sol)}} \overset{K_{ad}}{\rightleftarrows} O_{\text{(ads)}} \overset{k_s}{\underset{ne^-}{\rightleftarrows}} R_{\text{(sol)}} \tag{6}$$

$$R_{\text{(sol)}} + Y_{\text{(ex)}} \xrightarrow{k_{cat}} O_{\text{(sol)}} \tag{7}$$

where O corresponds to Cr(III)–DTPA, R to Cr(II)–DTPA, and Y to NO_3^-. Equations (6, 7) define an EC' reaction scheme, where E refers to the electrode reaction and C' indicates the irreversible chemical step that regenerates the reactant. In this particular case, the oxidized form of the electroactive species is supposed to be adsorbed and releases the reduced product to the solution. The electrochemical reaction of diverse metal complexes undergoes a similar adsorption/desorption scheme during their electrochemical reduction [16–21].

Recently, we developed a model for the catalytic adsorptive stripping response of square-wave voltammetry (SWV) described by Eqs. (6, 7); however, we were not able to match experimental results of Cr–DTPA with simulated curves [22]. Fortunately, there is another reaction scheme that has been used for describing the catalytic response of systems such as Co(III)/Co(II) and V(III)/V(II) in the presence of NO_2^- [23]. This mechanism is denominated catalytic system of second kind and can be described as follows [9]:

$$O_{\text{(sol)}} + Y_{\text{(sol)}} \overset{k_1'}{\underset{k_{-1}'}{\rightleftarrows}} P_{\text{(sol)}} \tag{8}$$

$$P_{\text{(sol)}} \overset{k_s'}{\underset{ne^-}{\rightleftarrows}} R_{\text{(sol)}} + Y_{\text{(sol)}} \tag{9}$$

Equation 9 indicates that only the complex P is electroactive, while the global reaction given by Eqs. (8, 9) points out that species O is consumed to produce R and that species Y works as the catalyzer. Here k_1' and k_{-1}' are second order homogeneous rate constants. However, since the concentration of nitrate ions is several orders of magnitude higher than that of chromium species, Eq. (8) can be simplified as a pseudo-first order reaction. In the present study, the voltammetric response of Cr–DTPA in the presence of nitrate is evaluated experimental and theoretically under SWV conditions.

The model

The mathematical model required for Eqs. (8, 9) is rather complex. However, according to the experimental conditions for the system Cr–DTPA, the concentration of nitrate is several orders of magnitude higher than that of the analyte. Thus, it can be assumed that the concentration of NO_3^- does not change at the electrode surface. This fact can be summarized as follows:

$$O_{\text{(sol)}} \overset{k_1}{\underset{k_{-1}}{\rightleftarrows}} P_{\text{(sol)}} \tag{10}$$

$$P_{\text{(sol)}} \overset{k_s}{\underset{ne^-}{\rightleftarrows}} R_{\text{(sol)}} \tag{11}$$

Equations (10, 11) correspond to a simple CE reaction mechanism [9, 24–26]. Here, k_1 and k_{-1} are the pseudo-first order homogeneous rate constants, the ratio $k_1 k_{-1}^{-1} = K$, which is the equilibrium constant for the complex formation of P species, and k_s is the charge transfer standard rate constant. Application of the second Fick's law to each of these species gives the following differential equations [24, 25]:

$$\partial c_O/\partial t = D(\partial^2 c_O/\partial x^2) - k_1 [c_O - c_P K^{-1}] \tag{12}$$

$$\partial c_P/\partial t = D(\partial^2 c_P/\partial x^2) + k_1 [c_O - c_P K^{-1}] \tag{13}$$

$$\partial c_R/\partial t = D(\partial^2 c_R/\partial x^2) \tag{14}$$

where a common diffusion coefficient value, $D = 4 \times 10^{-6}$ cm^2 s^{-1} is assumed for Eqs. (12, 13, and 14). Also, the following set of boundary conditions is considered:

$$t = 0, x = 0 : \quad c_O + c_P = c^* \quad ; c_O c_P^{-1} = K \tag{15}$$

$$c_R = 0 \tag{16}$$

$$t > 0, \quad x \to \infty : \quad c_O + c_P \to c^*; \quad c_O c_P^{-1} \to K \tag{17}$$

$$c_R \to 0 \tag{18}$$

$$x = 0 : \cdot D(\partial c_O/\partial x)_{x=0} = 0 \tag{19}$$

$$D(\partial c_P/\partial x)_{x=0} = -I/nFA \tag{20}$$

$$D(\partial c_R/\partial x)_{x=0} = I/nFA \tag{21}$$

$$I(t)/nFA = -k_s \exp[-\alpha\,\varphi(t)] \{(c_O)_{x=0} - (c_R)_{x=0}\exp[\varphi(t)]\} \tag{22}$$

$$\varphi(t) = nF[E(t) - E^{\circ\prime}]/RT \tag{23}$$

According to Eqs. (20, 21, and 22) the oxidation current is considered as positive. The parameter A is the electrode surface area, $E(t)$ is the square-wave potential function, $E^{\circ\prime}$ is the formal potential for a simple redox reaction, and other symbols have their usual meaning. The current is normalized according to:

$$\Psi(t) = I(t) \cdot \pi^{1/2} \left[nFAc^*(fD)^{1/2} \right]^{-1} \tag{24}$$

where f is the square-wave frequency. The following change of variables is required to solve the differential Eqs. (12, 13) [24]:

$$\phi = c_O + c_P \tag{25}$$

$$\theta = (c_O - c_P K^{-1})\exp(k_{chem}t) \tag{26}$$

The variable $k_{chem} = k_1 + k_{-1}$, is the cumulative rate constant of the coupled chemical reaction. After the change of variables, a new set of equations is obtained [24]:

$$\partial\phi/\partial t = D(\partial^2\phi/\partial x^2) \tag{27}$$

$$\partial\theta/\partial t = D(\partial^2\theta/\partial x^2) \tag{28}$$

$$D(\partial\phi/\partial x)_{x=0} = -I/nFA \tag{29}$$

$$D(\partial\theta/\partial x)_{x=0} = I\exp(k_{chem}t)/nFAK \tag{30}$$

The expression for the current is obtained by numerical integration [27]:

$$\Psi_{(m)} = \{\lambda\zeta + \zeta\,\Xi_{b(m)} + T_{(m)}\Xi_{a(m)}\}[-\aleph_{(m)} - \zeta\,Q_{(1)} - T_{(m)}]^{-1} \tag{31}$$

where $= K(K+1)^{-1}$; $\aleph_{(m)} = \mu\exp[\alpha\,\varphi_{(m)}]$; $\Xi_{a(m)} = \sum_{j=1}^{m-1}\Psi_{(j)}S_{(i)}$;

$\Xi_{b(m)} = \sum_{j=1}^{m-1}\Psi_{(j)}Q_{(i)}$; $S_{(i)} = (i)^{1/2} - (i-1)^{1/2}$; $i = m - j + 1$;

$Q_{(i)} = \{S_{(i)} + \gamma Y_{(i)}\}$; $Y_{(i)} = \mathrm{erf}[(k_{chem}\delta\,i)^{1/2}] - \mathrm{erf}[(k_{chem}\delta(i-1))^{1/2}]$; $\lambda = \pi(q/2)^{1/2}$; $T_{(m)} = \exp[\varphi_{(m)}]$; $\gamma = [\pi(k_{chem}\delta)^{-1}]^{1/2}(2K)^{-1}\mu = [D\pi\,\delta^{-1}]^{1/2}(2k_s)^{-1}$ and $\delta = (q\,f)^{-1}$. Here, q stands for the number of subintervals considered in each wave and a value of $q = 50$ has been employed for all calculations.

Experimental

All solutions were prepared with ultrapure water (18 MΩcm) from a Millipore MilliQ system. The solutions were buffered with 0.5 M acetic acid/Na acetate in 0.1 M KNO$_3$ (Sigma, Arg.), pH 6.5. Variable amounts of HNO$_3$ (Merck, Arg.) and KOH (Merck, Arg.) were used in order to adjust the pH to the desired value. The pH was checked before each experiment with a combined glass electrode. DTPA (Sigma, Arg.) solution was prepared by dissolving the appropriate amount of the reagent and the addition of 25 % ammonia (Suprapur, Merck, Arg.) until pH 6.0. A stock solution of Cr(VI) was prepared by dissolving K$_2$CrO$_4$ (Cicarelli, Arg.) in deionized water. All chemicals were reagent grade and used as received.

Solutions were degassed with high-purity nitrogen for 15 min prior to the measurements and for additional 20 s before each scan. A nitrogen atmosphere was maintained throughout the experiments. Each scan was done on a separate mercury drop at room temperature.

Measurements were performed with an Autolab (Eco-Chemie, Utrecht, Netherlands), equipped with a PSTAT 20 potentiostat and the GPES 4.3 software package. A static mercury drop (VA 663 Metrohm, Switzerland) with a surface area of 0.40 mm^2 was used as the working electrode. A glassy carbon rod was the counter electrode and all potentials in the text are referred to a Ag$_{(s)}$|AgCl$_{(s)}$|KCl$_{(aq)}$ (3 M) reference electrode.

Parameters in SWV experiments were defined as usual and reducing currents are considered to be negative [16–22, 25, 26]. In all cases, capacitive currents were subtracted.

Results and discussion

The electrochemical response of 0.3 μM Cr(III)–DTPA in the presence of 0.1 M KNO_3 is analyzed by cathodic stripping SWV. In all cases, cathodic scans are performed in 0.5 M acetate buffer at pH = 6.5 using a potential step (dE) = 5 mV. After extruding the mercury drop, a pre-concentration step under stirred conditions was applied during t_{ac} = 30 s at E_{ac} = −1.10 V. After a waiting period of 5 s in rest solution, the potential scan was started in the negative direction. The experimental results are compared with simulated curves calculated with Eq. (31). In all the cases, circles correspond to experimental data, while solid lines are theoretical curves.

It is well-known that the shape of voltammetric curves depends dramatically on the number of exchanged electrons [28]. Parameters such as the peak width at half height can decrease between 20 and 40 mV if a reaction exchanges 2 electrons instead of 1 electron [28]. The magnitude of this diminution depends on the square-wave amplitude (E_{sw}) used and on the reaction mechanism analyzed. However, once a feasible reaction mechanism has been selected, the first and simplest simulation step consists on determining the number of exchanged electrons. For the case of the electrochemical response of trace amounts of Cr(III)–DTPA in the presence of 0.1 M KNO_3, all experimental data can be fitted when the direct transfer of 2 electrons is considered. Besides, voltammetric experiments performed in the absence of nitrate ions give profiles that are identical to the baseline, not shown.

In Fig. 1, the forward and backward components of SWV experiments are presented together with simulated curves. Figure 1 (a–c) corresponds to different values of f, which is the parameter that determines the scan rate in SWV. Experimental voltammograms have been divided by $f^{1/2}$ to compare them with theoretical profiles, which are normalized according to Eq. (24). The reduction process assigned to the complex Cr–DTPA is observed in the potential range −1.5 V < E < −1.2 V. The shapes of the voltammetric curves evidence a rather slow charge transfer because the backward current does not present a peak. The effect of the coupled chemical reaction becomes more evident for the highest values of f [25]. In this regard, the peak of the normalized forward current decreases with the increment of f and the forward and backward components of current have shapes similar to sigmoid curves for f = 200 Hz, Fig. 1c. The peak potential (E_p) of the forward curve can be observed close to −1.34 V. However, the E_p value is not constant and shifts towards more negative potentials when f is increased. The
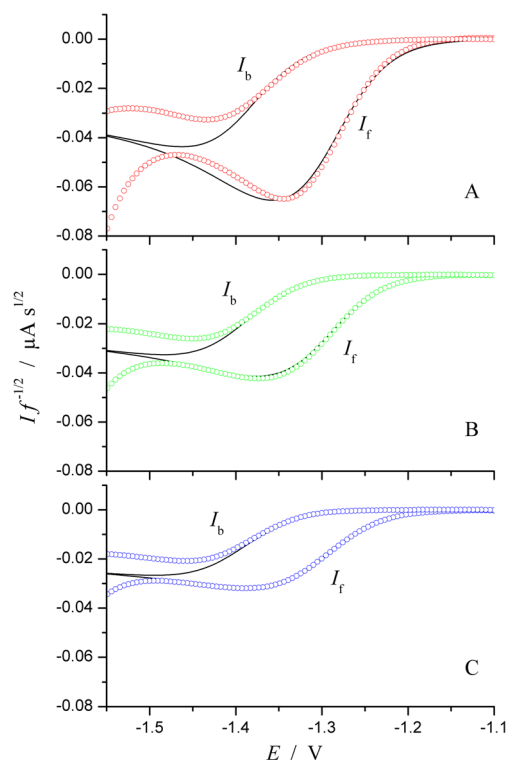

Fig. 1 Experimental (*circles*) and simulated (*lines*) SW voltammograms of the forward and backward components corresponding to K_2CrO_4 0.3 μM, DTPA 5 mM, KNO_3 0.1 M, pH = 6.5, t_{ac} = 30 s, and E_{ac} = −1.1 V. Theoretical results were calculated for k_s = 9.4 × 10^{-5} cm s^{-1}, k_{chem} = 1.3 × 10^4 s^{-1}, K = 0.01, α = 0.40, n = 2, $E°'$ = −1.098 V, E_{sw} = 50 mV, dE = 5 mV, and f/Hz = 25 (**a**), 75 (**b**), and 200 (**c**)

signal observed for E < −1.5 V corresponds to the reduction of protons to molecular hydrogen.

As already mentioned, lines in Fig. 1 correspond to simulated profiles obtained from Eq. (31). The experimental data have been divided by $f^{1/2}$ to simplify the comparison with normalized theoretical curves. As it can be observed, theoretical and experimental curves present very good correlation. Calculations were performed using the following parameters k_s = 9.4 × 10^{-5} cm s^{-1}, k_{chem} = 1.3 × 10^4 s^{-1}, K = 0.01, α = 0.40, n = 2, $E°'$ = −1.098 V, where the value of f was increased from 25 to 200 Hz for Fig. 1a to c, respectively. Besides the diverse parameters that result from simulated voltammograms, it is also necessary to calculate the scaling factor that transforms the dimensionless current into the measured current, Eq. (24). The scaling factor calculated for A = 0.004 cm^2, c^* = 0.3 μM, and D = 4 × 10^{-6} cm^2 s^{-1} is equal to 2.61 × 10^{-7} A s$^{1/2}$, which is very close to the value 3 × 10^{-7} A s$^{1/2}$ required to fit theoretical curves with experimental results. The minor difference between both scaling values would depend on the selected diffusion coefficient and eventually on the amount of adsorbed species. In this regard, it is important to keep in mind that the model does not consider the accumulation by adsorption of electroactive species. However, the very good fits achieved with theoretical curves point out that the adsorption

of reagents have to be rather weak. The simulations indicate also that 2 electrons are exchanged during the electrochemical step, which is a remarkable result. As a consequence of this, it might be advisable to reconsider the reaction mechanism proposed for the reduction of Cr–DTPA in the presence of nitrate.

Figure 2 shows experimental (circles) and simulated (lines) SW voltammograms corresponding to the response of the net current. These curves are obtained from the difference between the forward and backward components. As in the previous case, voltammetric profiles have been divided by $f^{1/2}$ to simplify the comparison with normalized theoretical curves. The simulated net currents consist on quite symmetric bell-shaped curves, while the net peak current decreases with the increment of f. Although this behavior was predicted more than a decade ago, it was rarely used to describe mechanistic aspects of the SWV response [25].

Figure 3 shows the dependence of $\Delta I_p f^{-1/2}$ (a) and E_p (b) with f. In both figures, the circles correspond to the experimental response of Cr–DTPA reduction in the presence of nitrate ions, while the lines connect the $\Delta I_p f^{-1/2}$ and E_p values of SW voltammograms calculated with Eq. (31). As it can be observed, there is excellent agreement between theoretical and experimental parameters. All theoretical net peak currents have been multiplied by the same scaling factor 3×10^{-7}.
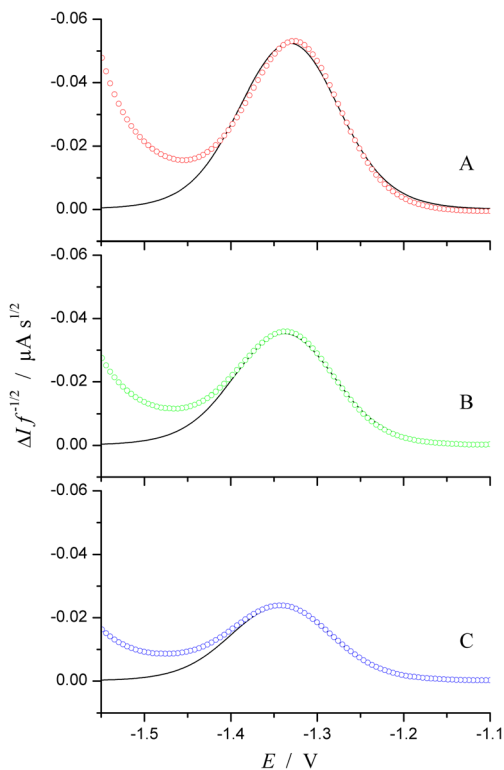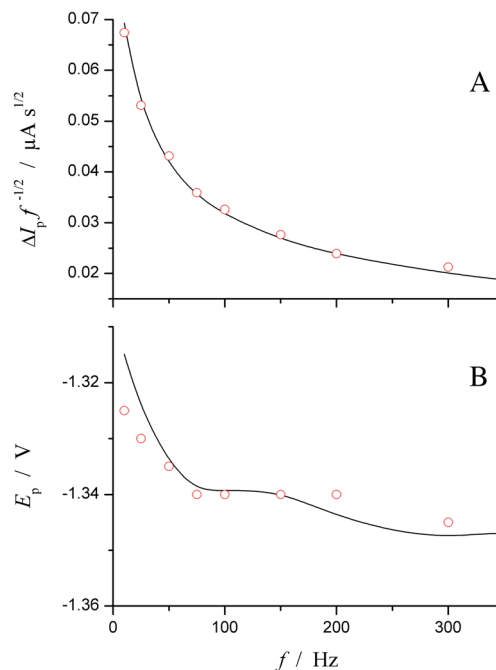

Fig. 3 Dependence of **a** $\Delta I_p f^{-1/2}$ and **b** E_p on f. *Circles* are experimental data obtained for K$_2$CrO$_4$ 0.3 μM, DTPA 5 mM, KNO$_3$ 0.1 M, pH = 6.5, t_{ac} = 30 s, and E_{ac} = −1.1 V. *Lines* connect theoretical results obtained for $k_s = 9.4 \times 10^{-5}$ cm s^{-1}, $k_{chem} = 1.3 \times 10^4$ s^{-1}, $K = 0.01$, $\alpha = 0.40$, $n = 2$, $E^{\circ\prime} = -1.098$ V, $E_{sw} = 50$ mV, and d$E = 5$ mV

Also, every SW voltametric profile was calculated with the same $E^{\circ\prime} = -1.098$ V. The rather complex dependence of E_p on f is the result of the joint effect of the chemical and electrochemical kinetics [25].

In Fig. 4, the net current of the SW voltammograms at different E_{sw} values are presented, as previously reported
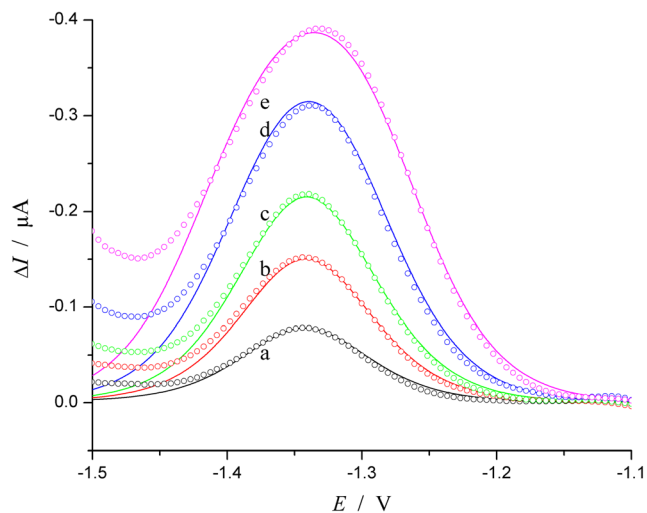

Fig. 2 Experimental (*circles*) and simulated (*lines*) differential SW voltammograms corresponding to K$_2$CrO$_4$ 0.3 μM, DTPA 5 mM, KNO$_3$ 0.1 M, pH = 6.5, t_{ac} = 30 s, and E_{ac} = −1.1 V. Theoretical results were calculated for $k_s = 9.4 \times 10^{-5}$ cm s^{-1}, $k_{chem} = 1.3 \times 10^4$ s^{-1}, $K = 0.01$, $\alpha = 0.40$, $n = 2$, $E^{\circ\prime} = -1.098$ V, $E_{sw} = 50$ mV, d$E = 5$ mV, and f/Hz = 25 (**a**), 75 (**b**), and 200 (**c**)

Fig. 4 Experimental (*circles*) and simulated (*lines*) SW voltammograms of the net component corresponding to K$_2$CrO$_4$ 0.3 μM, DTPA 5 mM, KNO$_3$ 0.1 M, pH = 6.5, t_{ac} = 30 s, and E_{ac} = −1.1 V. Theoretical results were calculated for $k_s = 9.4 \times 10^{-5}$ cm s^{-1}, $k_{chem} = 1.3 \times 10^4$ s^{-1}, $K = 0.01$, $\alpha = 0.40$, $n = 2$, $E^{\circ\prime} = -1.098$ V, $f = 100$ Hz, d$E = 5$ mV, and E_{sw}/mV = 10 (*a*), 20 (*b*), 30 (*c*), 50 (*d*), and 75 (*e*)

circles correspond to experimental results, while lines are the values of SW voltammograms calculated with Eq. (31). Although the symmetric bell-shaped curves of simulated net currents match very well the experimental profiles, the latter have a secondary signal for $E < -1.4$ V that overlaps with the main peak. This secondary process related to the reduction of protons introduces some errors on characteristic parameters of voltammetric peaks such as ΔI_p and E_p.

The dependences of $\Delta I_p E_{sw}^{-1}$ (a) and E_p (b) with E_{sw} are shown in Fig. 5. The line corresponding to simulated data fits very well the experimental responses of $\Delta I_p E_{sw}^{-1}$. With regard to the theoretical and experimental dependences of E_p on E_{sw}, the agreement is relatively good provided $E_{sw} < 75$ mV. For larger values of E_{sw}, the peaks are around 20 mV more positive than the theoretical value. This difference can be explained considering the association of the reduction process with hydrogen evolution reaction, since the overlap of both signals increases with the E_{sw} value. The values of thermodynamic parameters were the same than those obtained for previous figures and theoretical net peak currents have been multiplied by the same scaling factor 3×10^{-7}.
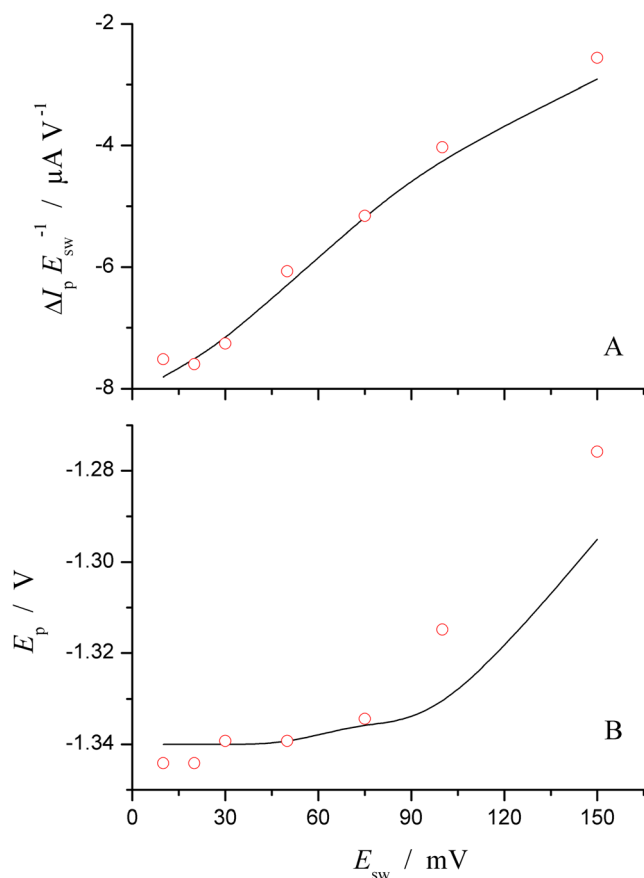
A secondary process such as the reduction of protons not only would affect ΔI_p and E_p values, but also it commonly introduces errors on the $\Delta E_{1/2}$ measurement. In this regard, Fig. 6 shows how most software used for the analysis of voltammetric responses measures the half peak width. However, it is important to keep in mind that the base line of the net current is not expected to be tilt in SWV. Thus, typical strategies for measuring the value of $\Delta E_{1/2}$ may introduce some errors as consequence of other signal that overlaps with the main peak. Those inaccuracies become evident when compared with results obtained from simulated curves, Fig. 6b. In consequence, it is suggested to measure the values of ΔI_p and $\Delta E_{1/2}$ assuming that the baseline is the same than the one recorded at the onset potential.

The comparison of experimental data with simulated curves would indicate that the reduction of Cr–DTPA in the presence of NO_3^- behaves according to a catalytic reaction of second kind in which 2 electrons are exchanged during the electrochemical step. As it was stated above, this kind of catalytic reaction is equivalent to a CE mechanism. The catalytic system involves a chemical reaction that generates the electroactive species P. In the case of Cr(III)–DTPA and NO_3^-, it should be considered that both species react to produce Cr(III)–NO_3–DTPA. Furthermore, it is well-known that Cr(III) forms diverse complexes with DTPA in aqueous solutions [15]. For most of those
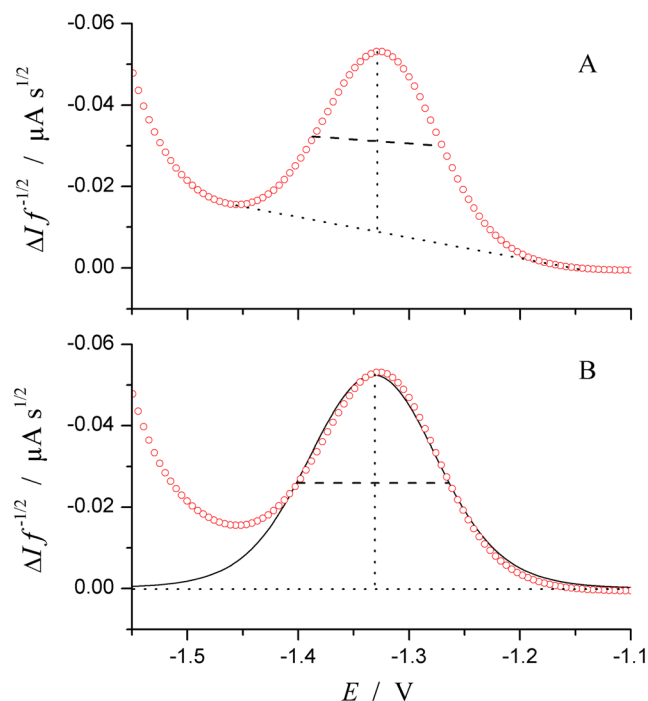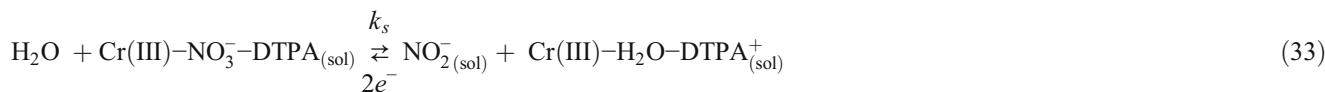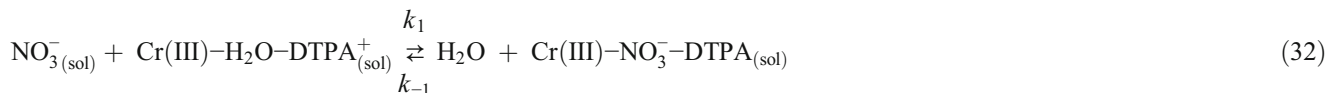

Fig. 5 Dependence of **a** $\Delta I_p E_{sw}^{-1}$ and **b** E_p on E_{sw}. *Circles* are experimental data obtained for K_2CrO_4 0.3 μM, DTPA 5 mM, KNO$_3$ 0.1 M, pH = 6.5, t_{ac} = 30 s, and E_{ac} = −1.1 V. *Lines* connect theoretical results obtained for k_s = 9.4 × 10^{-5} cm s^{-1}, k_{chem} = 1.3 × 10^4 s^{-1}, K = 0.01, α = 0.40, n = 2, $E°'$ = −1.098 V, f = 100 Hz, and dE = 5 mV

Fig. 6 Two different ways of measuring $\Delta E_{1/2}$. *Circles* are experimental data obtained for K_2CrO_4 0.3 μM, DTPA 5 mM, KNO$_3$ 0.1 M, pH = 6.5, t_{ac} = 30 s, and E_{ac} = −1.1 V. *Full line* connect theoretical results obtained for k_s = 9.4 × 10^{-5} cm s^{-1}, k_{chem} = 1.3 × 10^4 s^{-1}, K = 0.01, α = 0.40, n = 2, $E°'$ = −1.098 V, f = 100 Hz, E_{sw} = 50 mV, and dE = 5 mV

complexes, DTPA behaves as a pentadentate ligand, in which one iminodiacetic group remains free from coordination. Also, it has been suggested that in neutral solutions one molecule of water would be bound to the metal ion [15]. Thus, the intermediate species proposed in our model would involve the exchange of the water molecule by a nitrate anion. This reaction can be summarized according to the following mechanism:

$$NO_{3\,(sol)}^- + Cr(III){-}H_2O{-}DTPA_{(sol)}^+ \underset{k_{-1}}{\overset{k_1}{\rightleftarrows}} H_2O + Cr(III){-}NO_3^-{-}DTPA_{(sol)} \tag{32}$$

$$H_2O + Cr(III){-}NO_3^-{-}DTPA_{(sol)} \underset{2e^-}{\overset{k_s}{\rightleftarrows}} NO_{2\,(sol)}^- + Cr(III){-}H_2O{-}DTPA_{(sol)}^+ \tag{33}$$

where Cr(III)–H$_2$O–DTPA works as the catalyzer (Y) and NO$_3^-$ behaves as the substrate (O). Since NO$_3^-$ is in excess with regard to the concentration of Cr(III)–H$_2$O–DTPA, the analytical signal is controlled by the amount of catalyzer.

Conclusions

The reaction mechanism of Cr–DTPA in the presence of NO$_3^-$ has been evaluated. Experimental curves are in excellent agreement with theoretical profiles corresponding to a catalytic reaction of second kind, which is a reaction mechanism that is equivalent to a CE process. To understand this, it might be considered that the complex Cr(III)–H$_2$O–DTPA reacts with NO$_3^-$ to produce Cr(III)–NO$_3$–DTPA, in which the last species is the electroactive one. Since calculated curves require 2 electrons to fit experimental profiles, it is proposed that NO$_2^-$ is released to the solution as a product of the electrochemical step. In other words, the complex of Cr(III)–DTPA would work as catalyzer for the reduction of NO$_3^-$ to NO$_2^-$. Other results of simulations indicate that the electrochemical reaction is quite irreversible, with a value of $k_s = 9.4 \times 10^{-5}$ cm s^{-1}, while the chemical step has a value of $k_{chem} = 1.3 \times 10^4$ s^{-1}. Considering that $K = 0.01$, it is possible to estimate the kinetic constants of the chemical reaction as $k_1 = 1 \times 10^2$ s^{-1} and $k_{-1} = 1.29 \times 10^4$ s^{-1}. These values of k_1 and k_{-1} indicate a fast exchange of water molecules and nitrate ions where the equilibrium favors the complex with water. Also it was found that the value of $E°'$ is close to −1.1 V. Regardless experimental and simulated curves present very good fitting, the precision for kinetic and thermodynamic parameters determination, such as k_s, k_{chem}, α, and $E°'$, is limited. This is because similar profiles can be obtained by increasing one parameter and decreasing another. In this regard, it is important to keep in mind that the results of those calculations are restricted by confidence regions that depend on the interplay of involved variables [29]. To improve this, but not to avoid it, we are working on the inclusion of a non-linear least squares fitting protocol. This protocol will allow us to estimate the error of simulated data.

References

1. Espada-Bellido E, Bi Z, van den Berg CMG (2013) Talanta 105: 287–291
2. Ouyang R, Zhang W, Zhou S, Xue ZL, Xu L, Gu Y, Miao Y (2013) Electrochim Acta 113:686–693
3. Van den Berg CMG, Huang ZQ (1984) Anal Chem 56:2383–2386
4. Boussemart M, Van den Berg CMG, Ghaddaf M (1992) Anal Chim Acta 262:103–115
5. Biver M, Quentel F, Filella M (2015) Talanta 144:1007–1013
6. Caprara S, Laglera LM, Monticelli D (2015) Anal Chem 87:6357–6363
7. Vega M, Van den Berg CMG (1997) Anal Chem 69:874–881
8. Laglera LM, Santos-Echeandía J, Caprara S, Monticelli D (2013) Anal Chem 85:2486–2492
9. Mirčeski V, Bobrowski A, Zarebski J, Spasovski F (2010) Electrochim Acta 55:8696–8703
10. Bobrowski A, Baś B, Dominik J, Niewiara E, Szalińska E, Vignati D, Zarebski J (2004) Talanta 63:1003–1012
11. Li Y, Xue H (2001) Anal Chim Acta 448:121–134
12. Golimowski J, Valenta P, Nürnberg HW (1985) Fresenius' Z Anal Chem 322:315–322
13. Scholz F, Draheim M, Henrion G (1990) Fresenius J Anal Chem 336:136–138
14. Scholz F, Lange B, Pelzer DM (1990) Fresenius J Anal Chem 338: 627–629
15. Bucci R, Magri AL, Napoli A (1991) J Coord Chem 21:169–175
16. Lovrić M, Komorsky-Lovrić Š, Bond A (1991) J Electroanal Chem 319:1–18
17. Lovrić M (2013) J Chil Chem Soc 58:2191–2195
18. Garay F (2001) J Electroanal Chem 505:100–108
19. Garay F, Solis VM (2001) J Electroanal Chem 505:109–117
20. Garay F (2003) J Electroanal Chem 548:1–9

21. Garay F (2003) J Electroanal Chem 548:11–18
22. Vettorelo SN, Garay F (2016) J Solid State Elect. doi:10.1007/s10008-016-3273-9
23. Zarebski J, Bobrowski A, Królicka PM (2009) Collect Czech Chem Commun 74:1715–1725
24. Smith DE (1963) Anal Chem 35:602–609
25. Garay F, Lovrić M (2002) J Electroanal Chem 518:91–102
26. Mirčeski V, Komorsky-Lovrić S, Lovrić M (2007) In: Scholz F (ed) Square-wave voltammetry: theory and application. Heidelberg, Springer Verlag
27. Nicholson RS, Olmstead ML (1972) In: Mattson JS, Mark HB, MacDonald HC (eds) Electrochemistry: calculations, simulation and instrumentation, vol 2. New York, Marcel Dekker
28. Christie JH, Turner JA, Osteryoung RA (1977) Anal Chem 49:1899–1903
29. O'Dea JJ, Wikiel K, Osteryoung J (1990) J Phys Chem 94:3628–3636